

# UC Santa Barbara

## UC Santa Barbara Previously Published Works

### Title

Novel concept for ultracompact polarization splitter-rotator based on silicon nanowires

### Permalink

<https://escholarship.org/uc/item/98w3n3bb>

### Journal

Optics Express, 19(11)

### Authors

Dai, Daoxin  
Bowers, J E

### Publication Date

2011-05-20

Peer reviewed

# Novel concept for ultracompact polarization splitter-rotator based on silicon nanowires

Daoxin Dai<sup>1,2,\*</sup> and John E. Bowers<sup>1</sup>

<sup>1</sup>Department of Electrical and Computer Engineering, University of California, Santa Barbara, California 93106, USA

<sup>2</sup>Centre for Optical and Electromagnetic Research, State Key Laboratory for Modern Optical Instrumentation, Zhejiang Provincial Key Laboratory for Sensing Technologies, Zhejiang University, Zijingang Campus, Hangzhou 310058, China

\*dx dai@ece.ucsb.edu

**Abstract:** A novel concept for an ultracompact polarization splitter-rotator is proposed by utilizing a structure combining an adiabatic taper and an asymmetrical directional coupler. The adiabatic taper structure is singlemode at the input end while it becomes multimode at the other end. When light propagates along the adiabatic taper structure, the TM fundamental mode launched at the narrow end is efficiently (close to 100%) converted to the first higher-order TE mode at the wide end because of the mode coupling between them. By using an asymmetrical directional coupler that has two adjacent waveguides with different core widths, the first higher-order TE mode is then coupled to the TE fundamental mode of the adjacent narrow waveguide. On the other hand, the input TE polarization does not change when it goes through the adiabatic taper structure. In the region of the asymmetrical directional coupler, the TE fundamental mode in the wide waveguide is not coupled to the adjacent narrow waveguide because of phase mismatch. In this way, TE- and TM- polarized light are separated while the TM fundamental mode is also converted into the TE fundamental mode. A design example of the proposed polarization splitter-rotator is given by using silicon-on-insulator nanowires and the total length of the device is less than 100 $\mu\text{m}$ . Furthermore, only a one-mask process is needed for the fabrication process, which is compatible with the standard fabrication for the regular photonic integrated circuits based on SOI nanowires.

©2011 Optical Society of America

OCIS codes: (130.0130) Integrated optics; (230.5440) Polarization-selective devices.

---

## References and links

1. T. Barwicz, M. Watts, M. Popovic, P. Rakich, L. Socci, F. Kartner, E. Ippen, and H. Smith, "Polarization-transparent microphotonic devices in the strong confinement limit," *Nat. Photonics* **1**(1), 57–60 (2007).
2. K. Sasaki, F. Ohno, A. Motegi, and T. Baba, "Arrayed waveguide grating of  $70\times 60\mu\text{m}^2$  size based on Si photonic wire waveguides," *Electron. Lett.* **41**(14), 801–802 (2005).
3. D. Dai, L. Liu, L. Wosinski, and S. He, "Design and fabrication of ultra-small overlapped AWG demultiplexer based on alpha-Si nanowire waveguides," *Electron. Lett.* **42**(7), 400–402 (2006).
4. W. Bogaerts, S. K. Selvaraja, P. Dumon, J. Brouckaert, K. De Vos, D. Van Thourhout, and R. Baets, "Silicon-on-Insulator Spectral Filters Fabricated With CMOS Technology," *IEEE J. Sel. Top. Quantum Electron.* **16**(1), 33–44 (2010).
5. H. Fukuda, K. Yamada, T. Tsuchizawa, T. Watanabe, H. Shinjima, and S. Itabashi, "Silicon photonic circuit with polarization diversity," *Opt. Express* **16**(7), 4872–4880 (2008).
6. Z. Sheng, D. Dai, and S. He, "Comparative study of losses in ultrasharp silicon-on-insulator nanowire bends," *IEEE J. Sel. Top. Quantum Electron.* **15**(5), 1406–1412 (2009).
7. W. Bogaerts, P. Dumon, D. V. Thourhout, D. Taillaert, P. Jaenen, J. Wouters, S. Beckx, V. Wiaux, and R. G. Baets, "Compact wavelength-selective functions in silicon-on-insulator photonic wires," *IEEE J. Sel. Top. Quantum Electron.* **12**(6), 1394–1401 (2006).
8. D. Dai and S. He, "Design of a polarization-insensitive arrayed waveguide grating demultiplexer based on silicon photonic wires," *Opt. Lett.* **31**(13), 1988–1990 (2006).

9. D. Dai, Y. Shi, and S. He, "Theoretical Investigation for reducing polarization-sensitivity in Si-nanowire-based arrayed-waveguide grating (de)multiplexer with polarization-beam-splitters and reflectors," *IEEE J. Quantum Electron.* **45**(6), 654–660 (2009).
10. T. Pfau, R. Peveling, J. Hauden, N. Grossard, H. Porte, Y. Achiam, S. Hoffmann, S. K. Ibrahim, O. Adamczyk, S. Bhandare, D. Sandel, M. Pormann, and R. Noé, "Coherent digital polarization diversity receiver for real-time polarization-multiplexed QPSK transmission at 2.8 Gb/s," *IEEE Photon. Technol. Lett.* **19**(24), 1988–1990 (2007).
11. W. Bogaerts, D. Taillaert, P. Dumon, D. Van Thourhout, R. Baets, and E. Pluk, "A polarization-diversity wavelength duplexer circuit in silicon-on-insulator photonic wires," *Opt. Express* **15**(4), 1567–1578 (2007).
12. H. Fukuda, K. Yamada, T. Tsuchizawa, T. Watanabe, H. Shinjima, and S. Itabashi, "Ultrasmall polarization splitter based on silicon wire waveguides," *Opt. Express* **14**(25), 12401–12408 (2006).
13. M. A. Komatsu, K. Saitoh, and M. Koshiba, "Design of miniaturized silicon wire and slot waveguide polarization splitter based on a resonant tunneling," *Opt. Express* **17**(21), 19225–19233 (2009).
14. L. B. Soldano, A. I. de Vreede, M. K. Smit, B. H. Verbeek, E. G. Metaal, and F. H. Green, "Mach-Zehnder interferometer polarization splitter in InGaAsP-InP," *IEEE Photon. Technol. Lett.* **6**(3), 402–405 (1994).
15. T. K. Liang and H. K. Tsang, "Integrated polarization beam splitter in high index contrast silicon-on-insulator waveguides," *IEEE Photon. Technol. Lett.* **17**(2), 393–395 (2005).
16. W. W. Lui, T. Hirono, K. Yokoyama, and W.-P. Huang, "Polarization rotation in semiconductor bending waveguides: a coupled-mode theory formulation," *J. Lightwave Technol.* **16**(5), 929–936 (1998).
17. J. Zhang, M. B. Yu, G. Q. Lo, and D. L. Kwong, "Silicon-waveguide-based mode evolution polarization rotator," *IEEE J. Sel. Top. Quantum Electron.* **16**(1), 53–60 (2010).
18. N.-N. Feng, R. Sun, J. Michel, and L. C. Kimerling, "Low-loss compact-size slotted waveguide polarization rotator and transformer," *Opt. Lett.* **32**(15), 2131–2133 (2007).
19. Y. Yue, L. Zhang, M. Song, R. G. Beausoleil, and A. E. Willner, "Higher-order-mode assisted silicon-on-insulator 90 degree polarization rotator," *Opt. Express* **17**(23), 20694–20699 (2009).
20. B. M. A. Rahman, S. S. A. Obayya, N. Somasiri, M. Rajarajan, K. T. V. Grattan, and H. A. El-Mikathi, "Design and characterization of compact single-section passive polarization rotator," *J. Lightwave Technol.* **19**(4), 512–519 (2001).
21. H. H. Deng, D. O. Yevick, C. Brooks, and P. E. Jessop, "Design rules for slanted-angle polarization rotators," *J. Lightwave Technol.* **23**(1), 432–445 (2005).
22. Z. Wang and D. Dai, "Ultrasmall Si-nanowire-based polarization rotator," *J. Opt. Soc. Am. B* **25**(5), 747–753 (2008).
23. D. Vermeulen, S. Selvaraja, W. A. D. De Cort, N. A. Yebo, E. Hallynck, K. De Vos, P. P. P. Debackere, P. Dumon, W. Bogaerts, G. Roelkens, D. Van Thourhout, and R. Baets, "Efficient tapering to the fundamental Quasi-TM mode in asymmetrical waveguides," *ECIO 2010* (2010).
24. FIMMWAVE/FIMMPROP, Photon Design Ltd., <http://www.photond.com>.

## 1. Introduction

Silicon-on-insulator (SOI) waveguides [1–7] have become popular for photonic integrated circuits (PIC) because of their compatibility with mature CMOS technologies. SOI nanowires enable ultra-sharp bending (e.g., 1–2  $\mu\text{m}$ ) due to their ultra-high refractive index contrast [7]. Consequently various ultrasmall S-nanowire-based devices, e.g., arrayed-waveguide gratings (AWG) [2–4], microrings [5], etc. can be realized. However, it is well known that photonic integrated devices based on SOI nanowires are usually severely polarization-sensitive because of the huge structural birefringence [3], although it is often possible to diminish the polarization independence for some components by using approaches [8,9] that usually require a critical control for the waveguide dimension.

A general solution for the polarization issue is using a polarization diversity system consisting of polarization splitters and rotators [1,5]. Polarization diversity is also very important for many other applications, such as coherent receiver systems [10]. In Ref [11], a good design for a polarization diversity system was demonstrated to realize polarization-insensitive AWG by using two-dimensional grating coupler, which serves as a fiber-chip coupler, a polarization splitter as well as a rotator. However, it does not work for the case when the AWG is needed to be integrated with other components in the same chip.

Waveguide-type polarization splitters and polarization rotators are desired [12–15], but it is more difficult to realize waveguide-type polarization rotators because it is not easy to rotate the optical axis of a planar waveguide. In order to do that, one has to introduce some specific asymmetrical structures by using, e.g., off-axis double cores [5], cascaded bends [16], bi-level tapers [17,18], stacked waveguides [19], slanted cores [20,21], and cores with a cut corner [22]. These specific structures usually accompany complex and difficult fabrication, e.g., the

double etching process with critical requirement for the alignment, or the etching process to achieve a specific angle for the slanted sidewall.

In this paper, we propose a novel concept for a polarization diversity system including polarization splitting as well as rotation, which is realized by utilizing the structure consisting of an adiabatic taper and an asymmetrical directional coupler. The total length of the polarization diversity system is less than  $100\mu\text{m}$ . Furthermore, with the present concept, only one mask is needed for the fabrication of the designed polarization splitter-rotator, which makes the fabrication very simple.

## 2. Principle and structure design

We use a SOI wafer with  $h_{\text{co}} = 220\text{nm}$  and the refractive indices of Si and  $\text{SiO}_2$  are  $n_{\text{Si}} = 3.455$ , and  $n_{\text{SiO}_2} = 1.445$ , respectively. A finite-element method (FEM-FDM) mode solver (from COMSOL) is used to calculate the mode field profiles and the propagation constants for all eigenmodes.

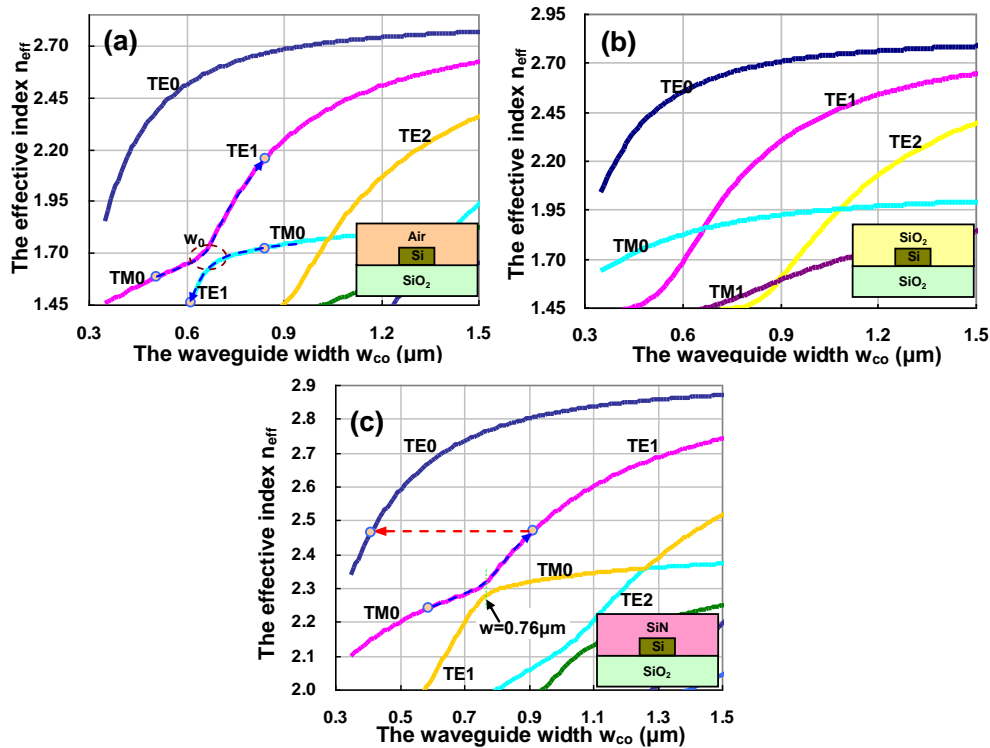


Fig. 1. The calculated effective indices for the eigen modes of SOI nanowires with different upper claddings. (a) Air cladding; (b)  $\text{SiO}_2$  cladding; (c)  $\text{Si}_3\text{N}_4$  cladding. Here the thickness of the Si core layer is  $h_{\text{co}} = 220\text{nm}$ .

Figure 1(a)–1(c) show the effective indices for a SOI nanowire as the core width  $w_{\text{co}}$  increases from  $0.3\mu\text{m}$  to  $1.5\mu\text{m}$  when the upper-cladding is air ( $n_{\text{cl}} = 1.0$ ),  $\text{SiO}_2$  ( $n_{\text{cl}} = 1.445$ ), and  $\text{Si}_3\text{N}_4$  ( $n_{\text{cl}} = 2.0$ ), respectively. When the upper-cladding is  $\text{SiO}_2$ , the SOI nanowire is vertically symmetrical and consequently the modes are purely polarized (as shown in Fig. 1(b)). On the other hand, when the upper-cladding index is not equal to that of the buffer layer ( $\text{SiO}_2$ ), the mode properties become more complicated as shown in Fig. 1(a), and Fig. 1(c). When choosing the core width in some special ranges labeled by circles, one cannot distinguish the polarization of some eigenmodes because of the mode hybridization. Such mode hybridization will introduce a mode conversion when light propagates along an adiabatic

taper structure. In Fig. 1(a) and Fig. 1(c), the dashed curves show the mode conversions between the TM fundamental mode and the first higher-order mode of TE polarization as the core width varies. Such a mode conversion is harmful when one expects to have a low-loss adiabatic taper structure [23]. In this paper we propose a structure to obtain a polarization rotator and splitter by utilizing the mode conversion.

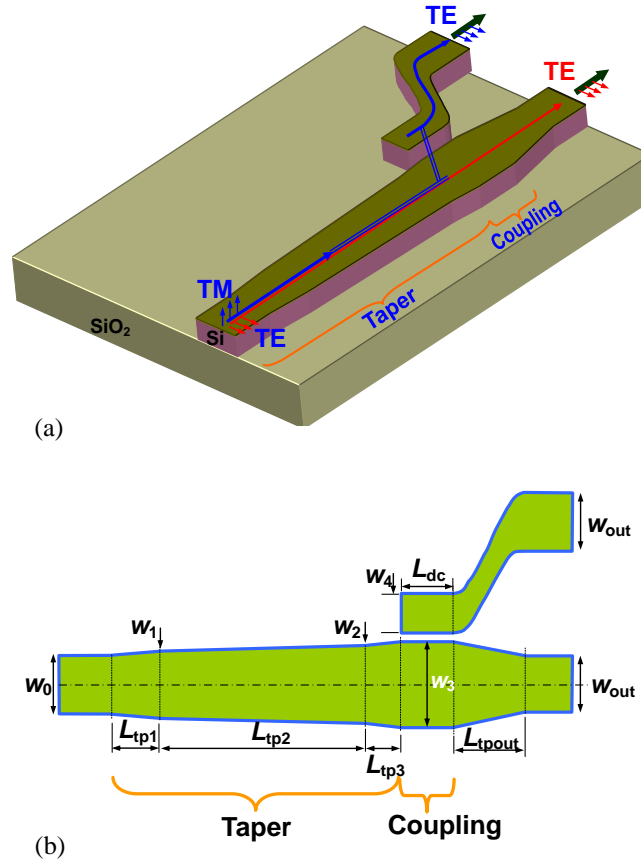


Fig. 2. The schematic configuration of the proposed polarization splitter-rotator based on an asymmetrical DC. (a) the 3D view; (b) the top view.

Figure 2 (a) and 2(b) show the three-dimensional view and the top view for the proposed ultracompact polarization splitter-rotator, which consists of a taper and an asymmetrical directional coupler. The taper structure is singlemode at the input end ( $w_0$ ) while it becomes multimode at the other end ( $w_3$ ). When light propagates along the taper structure, the TM fundamental mode launched at the narrow end ( $w_0$ ) is converted to the first higher-order TE mode at the wide end ( $w_3$ ) because of the mode coupling between them. Another narrow optical waveguide ( $w_4$ ) is then placed close to the wide waveguide ( $w_3$ ) and an asymmetrical directional coupler is formed. By using this asymmetrical directional coupler, the first higher-order TE mode in the wide waveguide is then coupled to the TE fundamental mode of the adjacent narrow waveguide. In this way, the input TM fundamental mode at the input waveguide is finally converted into the TE fundamental mode at the cross point of asymmetrical directional coupler. On the other hand, the input TE polarization keeps the same polarization state when it goes through the adiabatic taper structure. In the region of the asymmetrical directional coupler, the TE fundamental mode in the wide waveguide could not be coupled to the adjacent narrow waveguide because of the phase mismatching. In this way,

TE- and TM- polarized light are separated while the TM fundamental mode is also converted into TE fundamental mode.

In the following part, we consider the case of SOI nanowires with an upper-cladding of  $\text{Si}_3\text{N}_4$  in order to have a vertical asymmetry as well as to protect the waveguide. In order to obtain the mode conversion, the widths ( $w_0$ ,  $w_3$ ) at the two ends of the taper should be also chosen carefully according to the mode properties shown in Fig. 1(c). From Fig. 1(c), it can be seen that the mode conversion between the TM fundamental mode and the first higher-order TE mode happens in the domain around  $w = 0.76\mu\text{m}$ , where the gap between the two curves is smallest (see Fig. 1(c)). Therefore, we should make  $w_0 < 0.76\mu\text{m}$  and  $w_3 > 0.76\mu\text{m}$  for the ends of the taper. A smaller  $w_0$  and a larger  $w_3$  are desired to avoid the mode hybridization at the input section and the output section of the taper. Furthermore, the width  $w_0$  should be chosen to be singlemode. Therefore, we choose  $w_0 = 0.54\mu\text{m}$  (which is small enough to be singlemode, as shown in Fig. 1(c)), and  $w_3 = 0.9\mu\text{m}$  (which is far away from the mode coupling region, as shown in Fig. 1(c)).

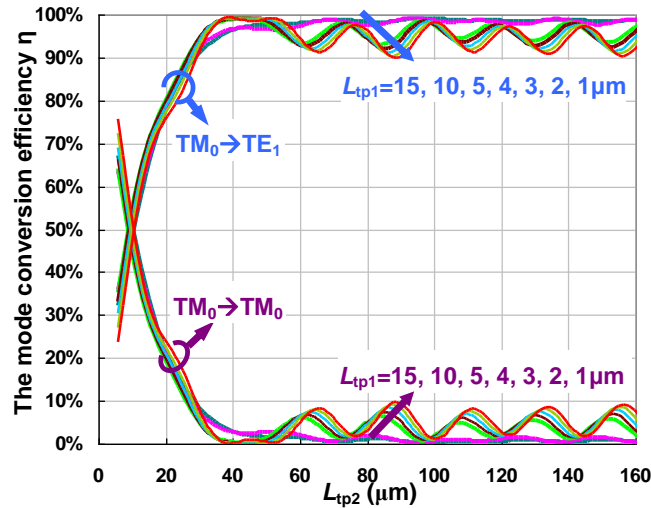


Fig. 3. The mode conversion efficiency  $\eta$  (from the  $\text{TM}_0$  mode to the  $\text{TE}_1$  mode) as  $L_{\text{tp}2}$  varies when TM fundamental mode is launched. Here the taper length  $L_{\text{tp}1} = 15, 10, 5, 4, 3, 2,$  and  $1\mu\text{m}$ . The taper length  $L_{\text{tp}3}$  is given by  $L_{\text{tp}3} = L_{\text{tp}1}(w_3 - w_2)/(w_1 - w_0)$ . The other parameters are  $w_0 = 0.54\mu\text{m}$ ,  $w_1 = 0.69\mu\text{m}$ ,  $w_2 = 0.83\mu\text{m}$ ,  $w_3 = 0.9\mu\text{m}$ .

In order to obtain a highly-efficient mode conversion, the taper length should be long enough to make the mode converted adiabatically. On the other hand, a short taper length is desired to make a compact device. For this sake, we design a three-segment taper, as shown in Fig. 2(b). The second segment should have a very small taper angle to be adiabatic and consequently to have a highly-efficient mode conversion. The end widths ( $w_1$ , and  $w_2$ ) for the second segment are chosen in the domain around  $w = 0.76\mu\text{m}$ , where the mode coupling happens. In the present design, we choose  $w_1 = 0.69\mu\text{m}$  and  $w_2 = 0.83\mu\text{m}$  as an example. The taper length ( $L_{\text{tp}2}$ ) for the second segment is then optimized for a maximized mode-conversion efficiency. For the first and the third segments, which won't influence the mode conversion greatly, the taper angles are relatively large to shorten the whole taper. In order to simplify the design, we choose different lengths for the first taper length (i.e.,  $L_{\text{tp}1} = 5, 10, 15,$  and  $20\mu\text{m}$ ) while the third taper length is given by  $L_{\text{tp}3} = L_{\text{tp}1}(w_3 - w_2)/(w_1 - w_0)$ . For any given taper length  $L_{\text{tp}1}$ , the taper length ( $L_{\text{tp}2}$ ) for the second segment is then optimized for a maximized mode-conversion efficiency. We use a commercial software (FIMMPROP, Photon Design, UK) employing an eigenmode expansion and matching method [24] to simulate the light propagation in the present structure. Figure 3 shows the mode conversion efficiencies to the TM fundamental mode and the first-order TE mode after the launched TM fundamental mode propagates along the three-segment taper structure. When the taper length  $L_{\text{tp}1}$  is short

(<10 $\mu\text{m}$ ), one sees that the curves ( $\eta \sim L_{\text{tp}2}$ ) have some notable ripples from Fig. 3. Fortunately one could still realize a very high efficiency (close to 100%) from the  $\text{TM}_0$  mode to the  $\text{TE}_1$  mode when choosing the taper length  $L_{\text{tp}2}$  appropriately for a given taper length  $L_{\text{tp}1}$ . On the other hand, when the taper length  $L_{\text{tp}1}$  is relatively large (>10 $\mu\text{m}$ ), the ripples becomes small. And the mode conversion efficiency becomes insensitive to the taper length  $L_{\text{tp}2}$  when  $L_{\text{tp}2}$  is large enough. This indicates that a larger fabrication tolerance, which will be shown below.

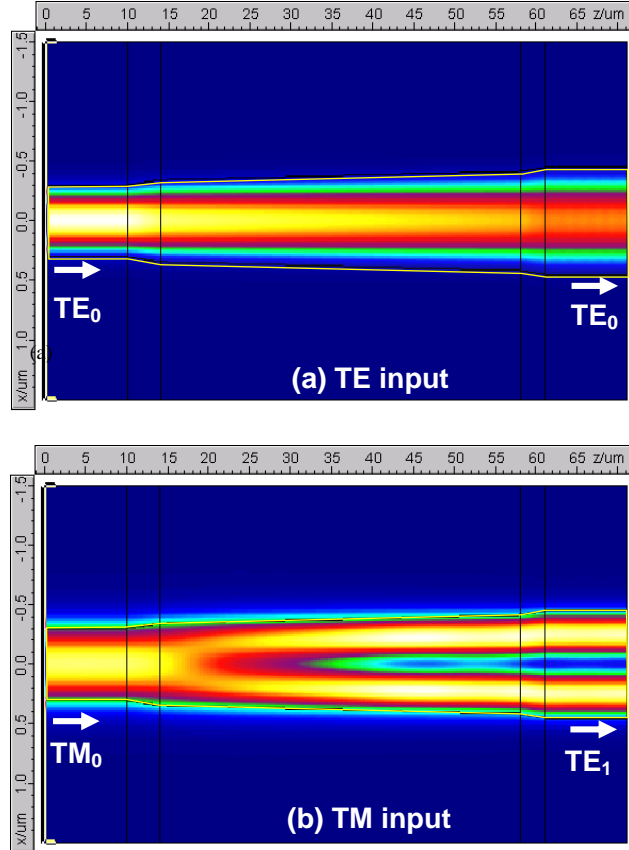


Fig. 4. The light propagation in the designed adiabatic taper when the input field is TE polarization (a), and TM polarization (b), respectively. Here the taper lengths are:  $L_{\text{tp}1} = 4\mu\text{m}$ ,  $L_{\text{tp}2} = 44\mu\text{m}$ , and  $L_{\text{tp}3} = L_{\text{tp}1}(w_3 - w_2)/(w_1 - w_0)$ . The other parameters are  $w_0 = 0.54\mu\text{m}$ ,  $w_1 = 0.69\mu\text{m}$ ,  $w_2 = 0.83\mu\text{m}$ , and  $w_3 = 0.9\mu\text{m}$ .

As an example, we choose  $L_{\text{tp}1} = 4\mu\text{m}$  and the corresponding optimal length  $L_{\text{tp}2} = 44\mu\text{m}$  for a compact device with a high  $\text{TM}_0$ - $\text{TE}_1$  mode conversion efficiency. Figure 4(a) and 4(b) show the simulation results for the intensity of light propagating along the designed taper, which were calculated by using a commercial software (FIMMPROP, Photon Design, UK). It can be seen that the mode conversion happens for the input TM fundamental as expected, while there is no mode conversion for the TE fundamental mode. In order to realize a polarization splitter-rotator, we put a narrow optical waveguide ( $w_4$ ) close to the output section of the adiabatic mode-conversion taper and then an asymmetrical directional coupler is formed, as shown in Fig. 2(a). This asymmetrical directional coupler is designed so that the first higher-order TE mode of the wide waveguide ( $w_3$ ) could be coupled to the TE fundamental mode of the narrow waveguide ( $w_4$ ). Thus, we choose the width of the adjacent narrow waveguide to make the phase matching condition satisfied, i.e.,  $n_{\text{effTE}0(2)} = n_{\text{effTE}1(1)}$ , where  $n_{\text{effTE}0(2)}$  is the effective index of the TE fundamental mode of the narrow waveguide ( $w_3$ ),  $n_{\text{effTE}1(1)}$  is the effective index of the first higher-order TE mode of the wide waveguide

( $w_4$ ). According to Fig. 1(c), the width of the adjacent narrow waveguide should be around  $w_4 = 0.405\mu\text{m}$ . Figure 5 shows the calculated coupling efficiency (at the central wavelength 1550nm) from the first higher-order TE mode of the wide waveguide ( $w_3 = 0.9\mu\text{m}$ ) to the TE fundamental mode of the narrow waveguide ( $w_4 = 0.405\mu\text{m}$ ). Here the gap width is chosen as 0.1, 0.15, 0.2, and 0.25 $\mu\text{m}$ , respectively. From this figure, one sees that there is the optimal coupling length for a maximal coupling efficiency and the optimal coupling length decreases as expected when the gap width decreases. For the sake of achieving a compact size as well as relatively easy fabrication, we choose  $w_{\text{gap}} = 0.15\mu\text{m}$ , and the corresponding coupling length is about  $L_{\text{dc}} = 7.0\mu\text{m}$ .

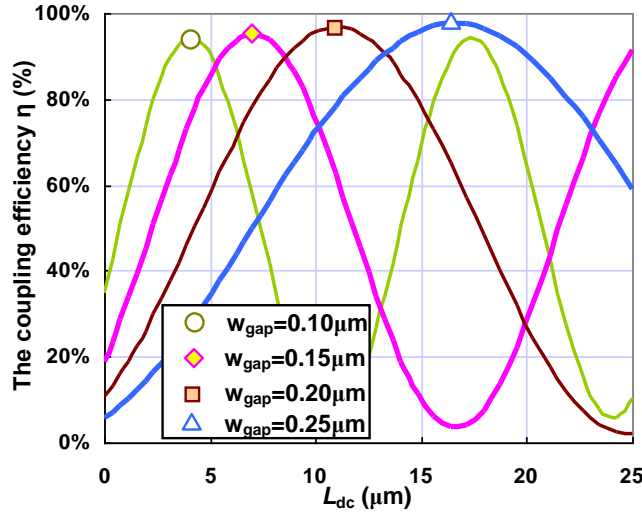


Fig. 5. The coupling efficiency from the first higher-order TE mode of the wide waveguide ( $w_3 = 0.9\mu\text{m}$ ) to the TE fundamental mode of the narrow waveguide ( $w_4 = 0.405\mu\text{m}$ ).

Figure 6(a) and 6(b) show the simulation results for the intensity of light propagating along the designed polarization splitter-rotator when choosing the optimal coupling length  $L_{\text{dc}} = 7.0\mu\text{m}$ . The widths of the output ports are tapered to be  $0.54\mu\text{m}$  at the end to be singlemode as well as be convenient to connect with other devices. One sees that the total length of the polarization splitter-rotator is about  $71\mu\text{m}$ . It can be seen that one obtains TE fundamental output from the cross port of the asymmetrical directional coupler when the TM fundamental mode is launched from the input port. On the other hand, for the input TE fundamental mode, because it could not be coupled to the adjacent narrow waveguide due to the phase mismatching, one obtains an output of TE fundamental mode at the through port. In this way, TE- and TM- polarized light are separated while the TM fundamental mode is also converted into the TE fundamental mode.

We also give an analysis for the fabrication tolerance and wavelength dependence of the designed polarization rotator-splitter. Figure 7(a) and 7(b) show wavelength dependence of the output powers at the cross port and the through port when the input is the TM fundamental mode ( $\text{TM}_0$ ), and the TE fundamental mode ( $\text{TE}_0$ ), respectively. From these figures, one sees that the output is not sensitive to the wavelength variation for the case when the TE fundamental mode ( $\text{TE}_0$ ) is launched. This is because the input  $\text{TE}_0$  mode has no mode conversion in the taper section and no coupling in the coupling region. In contrast, for the input TM fundamental mode, the response is sensitive to the wavelength, which is due to the wavelength dependences of the mode conversion in the taper region and the coupling in the coupling region. From Fig. 7(a), the designed polarization splitter-rotator has a relatively large bandwidth, which is more than 70nm for an extinction ratio of 10dB.



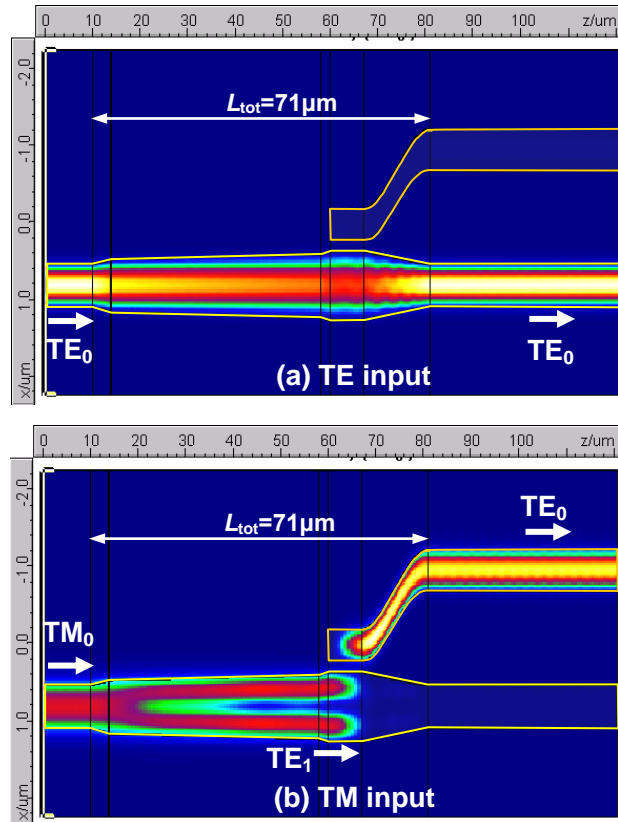


Fig. 6. The light propagation in the designed polarization splitter-rotator when the input field is TE polarization (a), and TM polarization (b). Here the taper lengths are:  $L_{tp1} = 4\mu\text{m}$ ,  $L_{tp2} = 44\mu\text{m}$ , and  $L_{tp3} = L_{tp1}(w_3 - w_2)/(w_1 - w_0)$ . The other parameters are  $w_0 = 0.54\mu\text{m}$ ,  $w_1 = 0.69\mu\text{m}$ ,  $w_2 = 0.83\mu\text{m}$ ,  $w_3 = 0.9\mu\text{m}$ ,  $w_{\text{gap}} = 0.15\mu\text{m}$ , and  $L_{dc} = 7.0\mu\text{m}$ .

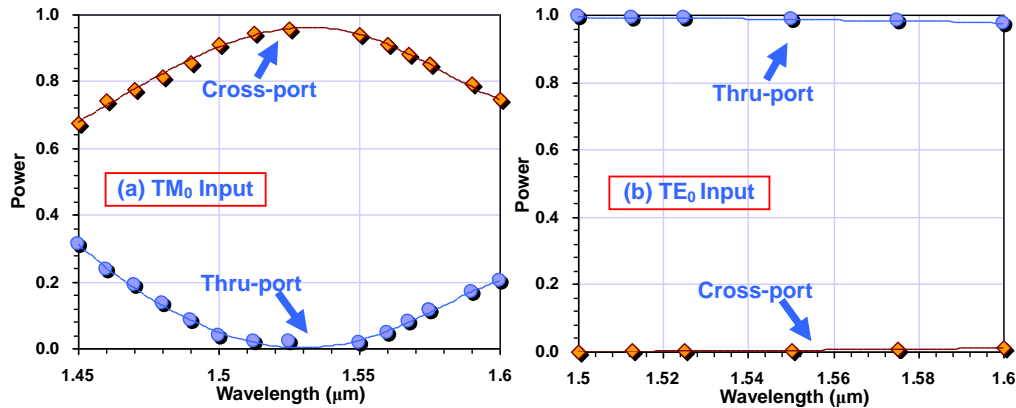


Fig. 7. The wavelength dependence of the designed polarization rotator-splitter when the input is: (a) the TM fundamental mode ( $\text{TM}_0$ ), and (b) the TE fundamental mode ( $\text{TE}_0$ ).

Figure 8(a) and 8(b) show the output powers at the cross port and the through port for the cases with a deviation of waveguide widths when the input is the TM fundamental mode ( $\text{TM}_0$ ), and the TE fundamental mode ( $\text{TE}_0$ ), respectively. For the case with a  $\text{TE}_0$  input, it can be seen that the responses change very slightly when there is a fabrication error as large as  $\pm$

40nm. The reason is the same as that for the wavelength-insensitivity shown in Fig. 7(b). In contrast, when the TM fundamental mode is launched, the response is sensitive to the width deviation  $\Delta w$  because the mode conversion in the taper region and the coupling in the coupling region are sensitive to the fabrication error  $\Delta w$ . From Fig. 8(a), the tolerance for the width deviation is about  $-10\text{nm} < \Delta w < 20\text{nm}$  for an extinction ratio of 10dB.

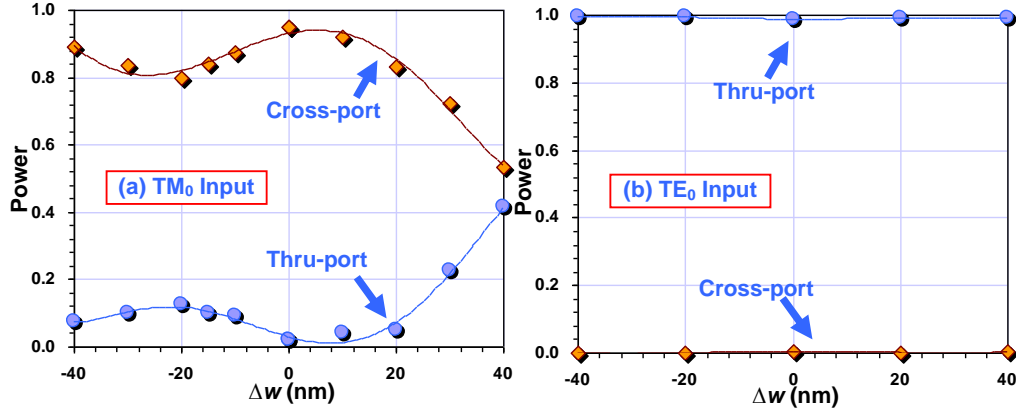


Fig. 8. The fabrication tolerance of the designed polarization rotator-splitter when the input is: (a) the TM fundamental mode ( $\text{TM}_0$ ), and (b) the TE fundamental mode ( $\text{TE}_0$ ).

Since the ripples of the curves ( $\eta \sim L_{\text{tp}2}$ ) shown in Fig. 3 become small when the taper length  $L_{\text{tp}1}$  is relatively large ( $>10\mu\text{m}$ ), we expect to achieve a larger bandwidth and fabrication tolerance by choosing longer tapers. As an example, we choose the following parameters for the polarization splitter-rotator with a longer taper: the taper lengths  $L_{\text{tp}1} = 10\mu\text{m}$ ,  $L_{\text{tp}2} = 69\mu\text{m}$ , and  $L_{\text{tp}3} = L_{\text{tp}1}(w_3 - w_2)/(w_1 - w_0)$ . The other parameters are the same as that used in Fig. 7 and Fig. 8, i.e.,  $w_0 = 0.54\mu\text{m}$ ,  $w_1 = 0.69\mu\text{m}$ ,  $w_2 = 0.83\mu\text{m}$ ,  $w_3 = 0.9\mu\text{m}$ ,  $w_{\text{gap}} = 0.15\mu\text{m}$ , and  $L_{\text{dc}} = 7.0\mu\text{m}$ . Since the response of the device for the case with the  $\text{TE}_0$  input is not sensitive to the wavelength as well as the waveguide width variations, here we show the results for the case with a  $\text{TM}_0$  input only. The wavelength dependence and the fabrication tolerance for this design with the longer taper are shown in Fig. 9(a) and 9(b), respectively. For a 10dB extinction ratio, the bandwidth is more than 130nm and the tolerance for the width deviation is about  $-40\text{nm} < \Delta w < 30\text{nm}$ .

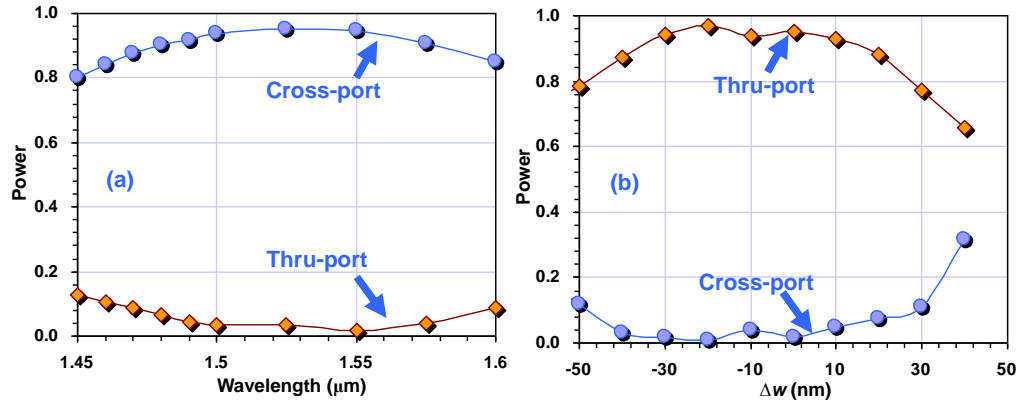


Fig. 9. (a) The wavelength dependence, and (b) the fabrication tolerance of the designed polarization rotator-splitter with a longer taper. The input is the TM fundamental mode ( $\text{TM}_0$ ). The taper lengths  $L_{\text{tp}1} = 10\mu\text{m}$ ,  $L_{\text{tp}2} = 69\mu\text{m}$ , and  $L_{\text{tp}3} = L_{\text{tp}1}(w_3 - w_2)/(w_1 - w_0)$ .

### 3. Conclusions

In this paper, we have proposed a novel concept for an ultracompact polarization splitter-rotator by utilizing a structure combining an adiabatic taper and an asymmetrical directional coupler. When light propagates along the adiabatic taper structure, the TM fundamental mode launched at the narrow end is converted to the first higher-order TE mode at the wide end because of the mode coupling between them. The theoretical mode conversion efficiency is close to 100%. By using an asymmetrical directional coupler which has two adjacent waveguides with different core widths, the first higher-order TE mode is then coupled to the TE fundamental mode of the adjacent narrow waveguide. On the other hand, the input TE polarization does not change when it goes through the adiabatic taper structure. In the region of the asymmetrical directional coupler, the TE fundamental mode in the wide waveguide could not be coupled to the adjacent narrow waveguide because of the phase mismatching. In this way, TE- and TM- polarized light are separated while the TM fundamental mode is also converted into the TE fundamental mode. We have presented an example of designing the proposed polarization splitter-rotator by using SOI nanowires and the total length of the whole polarization diversity device is less than 100 $\mu$ m. Furthermore, only a one-mask process is needed for the fabrication process, which is compatible with the standard fabrication for the regular photonic integrated circuits based on SOI nanowires. The proposed concept could be also be used for the platforms based on other materials.

### Acknowledgments

This research is supported by DARPA MTO under the CIPhER contract No: HR0011-10-1-0079. The authors thank Scott Rodgers for useful discussions.